

Time-integrated measurements of the CKM angle  $\gamma/\phi_3$  in  
*BABAR*

GIOVANNI MARCHIORI<sup>1</sup>  
ON BEHALF OF THE *BABAR* COLLABORATION

*Laboratoire de Physique Nucléaire et de Hautes Energies  
IN2P3/CNRS, F-75252 Paris, FRANCE*

The most recent determinations of the CKM angle  $\gamma/\phi_3$  by the *BABAR* Collaboration, using time-integrated observables measured in charged  $B \rightarrow D^{(*)}K^{(*)}$  decays, are presented. The measurements have been performed on the full sample of 468 million  $B\bar{B}$  pairs collected by the *BABAR* detector at the SLAC PEP-II asymmetric-energy  $B$  factory in the years 1999-2007.

PROCEEDINGS OF

CKM2010, the 6th International Workshop on the CKM  
Unitarity Triangle  
University of Warwick, UK  
6-10 September 2010

---

<sup>1</sup>e-mail: giovanni.marchiori@lpnhe.in2p3.fr

# 1 Introduction

A theoretically clean measurement of the angle  $\gamma \equiv \arg \left[ -\frac{V_{ud}V_{ub}^*}{V_{cd}V_{cb}^*} \right]$  (also denoted as  $\phi_3$  in the literature) can be obtained using  $CP$ -violating  $B \rightarrow D^{(*)}K^{(*)}$  decays. The interference between the  $b \rightarrow c\bar{u}s$  and  $b \rightarrow u\bar{c}s$  tree amplitudes results in observables that depend on the relative weak phase  $\gamma$ , the magnitude ratio  $r_B \equiv \left| \frac{A(b \rightarrow u)}{A(b \rightarrow c)} \right|$ , and the relative strong phase  $\delta_B$  between the two amplitudes. The hadronic parameters,  $r_B$  and  $\delta_B$ , depend on the  $B$  decay under investigation; they can not be precisely calculated from theory, but can be extracted directly from data by simultaneously reconstructing several different  $D$  final states.

In this contribution we present the most recent  $\gamma$  determinations obtained by *BABAR*, based on the full sample ( $\approx 468 \times 10^6$   $B^\pm$  decays) of charged  $B$  mesons produced in  $e^+e^- \rightarrow \Upsilon(4S) \rightarrow B^+B^-$  and accumulated in the years 1999-2007. The following decays have been reconstructed: (i)  $B^\pm \rightarrow D^{(*)}K^\pm$  and  $B^\pm \rightarrow DK^{*\pm}$  ( $K^{*\pm} \rightarrow K_s^0\pi^\pm$ ), with  $D \rightarrow K_s^0h^+h^-$ ,  $h = \pi, K$ ; (ii)  $B^\pm \rightarrow DK^\pm$ , with  $D$  decaying to  $CP$ -eigenstates  $f_{CP}$ ; (iii)  $B^\pm \rightarrow D^{(*)}K^\pm$ , with  $D$  decaying to  $K^\pm\pi^\mp$ . The results are statistically limited, as the effects that are being searched for are tiny, since: (i) the branching fractions of the  $B$  meson decays considered here are on the order of  $5 \times 10^{-4}$  or lower; (ii) the branching fractions for  $D^{(*)}$  decays, including secondary decays, range between  $O(10^{-2})$  and  $O(10^{-4})$ ; (iii) the interference between the  $b \rightarrow c$  and  $b \rightarrow u$  mediated  $B$  decay amplitudes is low, as the ratios  $r_B$  are around 0.1 due to CKM factors and the additional color-suppression of  $A(b \rightarrow u)$ .

The  $B$  decay final states are completely reconstructed, with efficiencies between 40% (for low-multiplicity, low-background decay modes) and 5% (for high-multiplicity decays). The selection is optimized to maximise the statistical sensitivity  $S/\sqrt{S+B}$ , where the number of expected signal ( $S$ ) and background ( $B$ ) events is estimated from simulated samples and data control samples. Signal  $B$  decays are distinguished from  $B\bar{B}$  and continuum  $q\bar{q}$  background by means of maximum likelihood fits to two variables exploiting the kinematic constraint from the known beam energies: the energy-substituted invariant mass  $m_{ES} \equiv \sqrt{E_{\text{beam}}^{*2} - p_B^{*2}}$  and the energy difference  $\Delta E \equiv E_B^* - E_{\text{beam}}^*$ . Additional continuum background discrimination is achieved by including in the likelihood a variable built, using multivariate analysis tools, from the combination (either a linear Fisher discriminant,  $\mathcal{F}$ , or a non-linear neural-network,  $NN$ ) of several event-shape quantities. These variables distinguish spherical  $B\bar{B}$  events from more jet-like  $q\bar{q}$  events and exploit the different angular correlations in the two event categories.  $B \rightarrow D^{(*)}\pi$  decays, which are 12 times more abundant than  $B \rightarrow D^{(*)}K$  and are expected to show negligible  $CP$ -violating effects ( $r_B \approx 0.01$  in such decays), are discriminated by means of the excellent pion and kaon identification provided by  $dE/dx$  measured in the charged particle tracking devices and by the radiation detected in the Cherenkov detector, and are used as control samples.

## 2 Dalitz-plot method: $B^\pm \rightarrow D^{(*)}K^{(*)\pm}, D \rightarrow K_S^0 h^+ h^-$

We reconstruct  $B^\pm \rightarrow DK^\pm, D^*K^\pm$  ( $D^* \rightarrow D\gamma$  and  $D\pi^0$ ), and  $DK^{*\pm}$  ( $K^{*\pm} \rightarrow K_S^0\pi^\pm$ ) decays, followed by neutral  $D$  meson decays to the 3-body self-conjugate final states  $K_S^0 h^+ h^-$  ( $h = \pi, K$ ) [1]. From an extended maximum likelihood fit to  $m_{ES}, \Delta E$  and  $\mathcal{F}$  (Fig. 1) we determine the signal and background yields in each channel: we find 268  $B$  candidates with  $D \rightarrow K_S^0 K^+ K^-$  and 1507  $B$  candidates with  $D \rightarrow K_S^0 \pi^+ \pi^-$ .

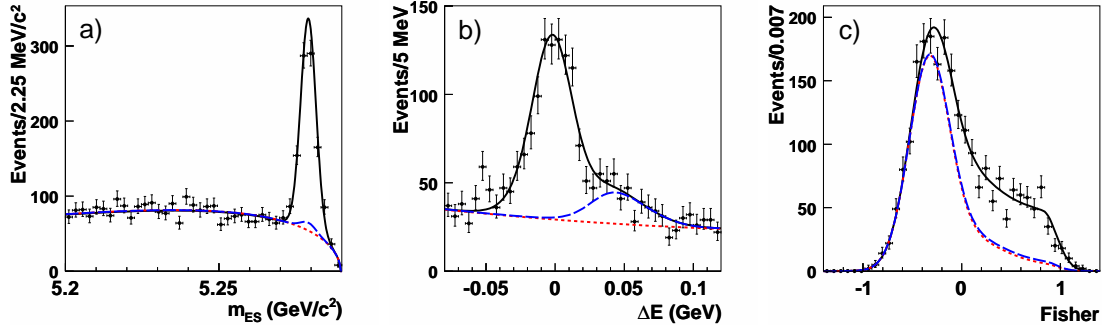


Figure 1: The  $m_{ES}$  (a),  $\Delta E$  (b), and  $\mathcal{F}$  (c) distributions for  $B^\pm \rightarrow DK^\pm, D \rightarrow K_S^0 \pi^+ \pi^-$ , for events in the signal region ( $m_{ES} > 5.272$   $\text{GeV}/c^2$ ,  $|\Delta E| < 30$   $\text{MeV}$ , and  $\mathcal{F} > -0.1$ ), after all the selection criteria, except the one on the plotted variable, are applied. The curves represent the fit projections: signal plus background (solid black lines),  $q\bar{q} + B\bar{B}$  background (dotted red lines),  $q\bar{q} + B\bar{B} + B \rightarrow D\pi$  background (dashed blue lines).

Following the technique proposed in [2], from a fit to the Dalitz-plot distribution of the  $D$  daughters we determine 2D confidence regions for the variables  $x_\pm \equiv r_B \cos(\delta_B \pm \gamma)$  and  $y_\pm \equiv r_B \sin(\delta_B \pm \gamma)$  (Fig. 2). In the fit we model the  $D^0$  and  $\bar{D}^0$  decay amplitudes to  $K_S^0 h^+ h^-$  as the coherent sum of a non-resonant part and several intermediate two-body decays that proceed through known  $K_S^0 h$  or  $h^+ h^-$  resonances. The model is determined from large ( $\approx 6.2 \times 10^5$ ) and very pure ( $\approx 99\%$ ) control samples of  $D$  mesons produced in  $D^* \rightarrow D\pi$  decays [3]. The results for  $x$  and  $y$  are summarized in Table 1.

Parameter	$B^\pm \rightarrow DK^\pm$	$B^\pm \rightarrow D^*K^\pm$	$B^\pm \rightarrow DK^{*\pm}$
$x_+$	$-0.103 \pm 0.037 \pm 0.006 \pm 0.007$	$0.147 \pm 0.053 \pm 0.017 \pm 0.003$	$-0.151 \pm 0.083 \pm 0.029 \pm 0.006$
$y_+$	$-0.021 \pm 0.048 \pm 0.004 \pm 0.009$	$-0.032 \pm 0.077 \pm 0.008 \pm 0.006$	$0.045 \pm 0.106 \pm 0.036 \pm 0.008$
$x_-$	$0.060 \pm 0.039 \pm 0.007 \pm 0.006$	$-0.104 \pm 0.051 \pm 0.019 \pm 0.002$	$0.075 \pm 0.096 \pm 0.029 \pm 0.007$
$y_-$	$0.062 \pm 0.045 \pm 0.004 \pm 0.006$	$-0.052 \pm 0.063 \pm 0.009 \pm 0.007$	$0.127 \pm 0.095 \pm 0.027 \pm 0.006$

Table 1: Values of  $x_\pm$  and  $y_\pm$  measured with the Dalitz-plot analysis of  $B^\pm \rightarrow D^{(*)}K^{(*)\pm}$

From the  $(x_\pm, y_\pm)$  confidence regions we determine, using a frequentist procedure,  $1\sigma$  confidence intervals for  $\gamma, r_B$  and  $\delta_B$  (Fig. 3). We obtain  $\gamma \bmod 180^\circ = (68 \pm 14 \pm$

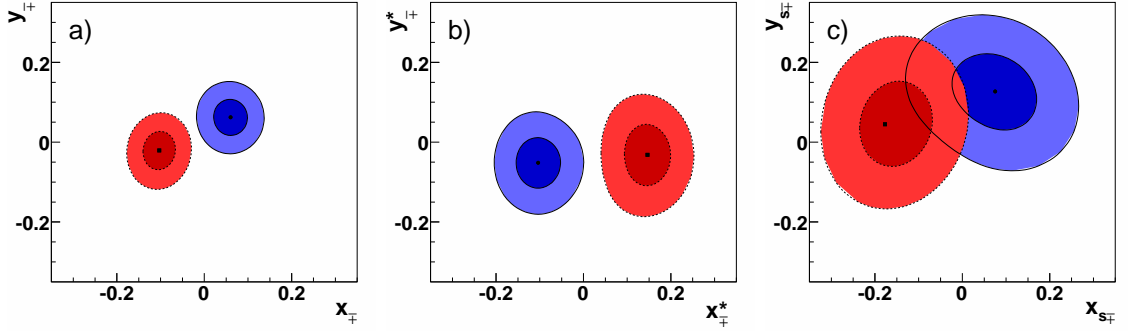


Figure 2:  $1\sigma$  and  $2\sigma$  contours in the  $x_{\pm}, y_{\pm}$  planes for (a)  $B \rightarrow DK$ , (b)  $B \rightarrow D^*K$  and (c)  $B \rightarrow DK^*$ , for  $B^-$  (solid lines) and  $B^+$  (dotted lines) decays.

$4 \pm 3)^\circ$ , where the three uncertainties are respectively the statistical, the experimental systematic and the Dalitz-model systematic ones. We find values of  $r_B$  around 0.1, confirming that interference is low in these channels:  $r_B^{DK^\pm} = 0.096 \pm 0.029$ ;  $r_B^{D^*K^\pm} = 0.133^{+0.042}_{-0.039}$ ;  $kr_B^{DK^{*\pm}} = 0.149^{+0.066}_{-0.062}$  ( $k=0.9 \pm 0.1$  takes into account the  $K^*$  finite width). We also measure the strong phases (modulo  $180^\circ$ ):  $\delta_B^{DK^\pm} = (119^{+19}_{-20})^\circ$ ;  $\delta_B^{D^*K^\pm} = (-82 \pm 21)^\circ$ ;  $\delta_B^{DK^{*\pm}} = (111 \pm 32)^\circ$ . A  $3.5\sigma$  evidence of direct  $CP$  violation is found from the distance between  $(x_+, y_+)$  and  $(x_-, y_-)$  (0 in absence of  $CPV$ ) in the three  $B$  decay channels.

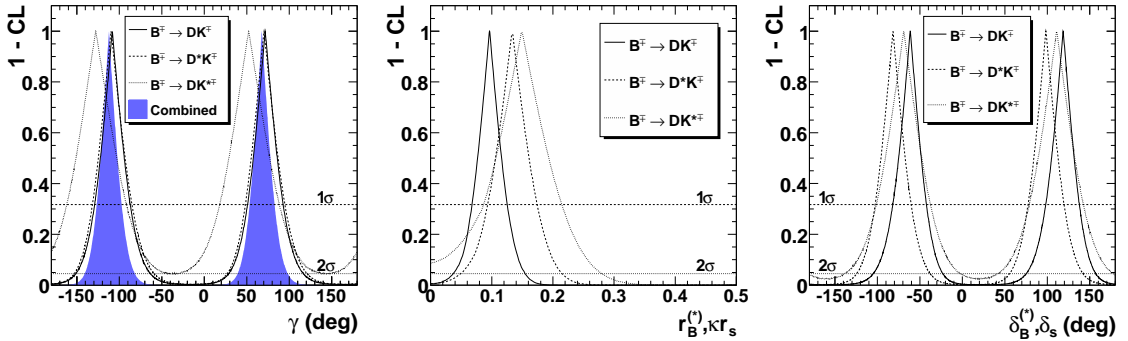


Figure 3: 1-confidence level (CL) as a function of  $\gamma$  (left),  $r_B$  (center) and  $\delta_B$  (right) from the  $B \rightarrow D^{(*)}K^{(*)}$  Dalitz-plot analysis.

### 3 GLW method: $B^\pm \rightarrow DK^{(*)\pm}$ , $D \rightarrow f_{(CP)}$

We reconstruct  $B^\pm \rightarrow DK^\pm$  decays, with  $D$  mesons decaying to non- $CP$  ( $D^0 \rightarrow K^- \pi^+$ ),  $CP$ -even ( $K^+ K^-, \pi^+ \pi^-$ ) and  $CP$ -odd ( $K_s^0 \pi^0, K_s^0 \phi, K_s^0 \omega$ ) eigenstates [4].

The partial decay rate charge asymmetries  $A_{CP\pm}$  for  $CP$ -even and  $CP$ -odd  $D$  final states and the ratios  $R_{CP\pm}$  of the charged-averaged  $B$  meson partial decay rates in  $CP$  and non- $CP$  decays provide a set of four observables from which the three unknowns  $\gamma$ ,  $r_B$  and  $\delta_B$  can be extracted (with an 8-fold discrete ambiguity for the phases) [5].

The signal yields, from which the partial decay rates are determined, are obtained from maximum likelihood fits to  $m_{ES}$ ,  $\Delta E$  and  $\mathcal{F}$ . An example is shown in Fig. 4. We identify about 500  $B^\pm \rightarrow DK^\pm$  decays with  $CP$ -even  $D$  final states and a similar amount of  $B^\pm \rightarrow DK^\pm$  decays with  $CP$ -odd  $D$  final states. We measure  $A_{CP+} = 0.25 \pm 0.06 \pm 0.02$  and  $A_{CP-} = -0.09 \pm 0.07 \pm 0.02$ , respectively, where the first error is the statistical and the second is the systematic uncertainty. The parameter  $A_{CP+}$  is different from zero with a significance of 3.6 standard deviations, constituting evidence for direct  $CP$  violation. We also measure  $R_{CP+} = 1.18 \pm 0.09 \pm 0.05$  and  $R_{CP-} = 1.07 \pm 0.08 \pm 0.04$ .

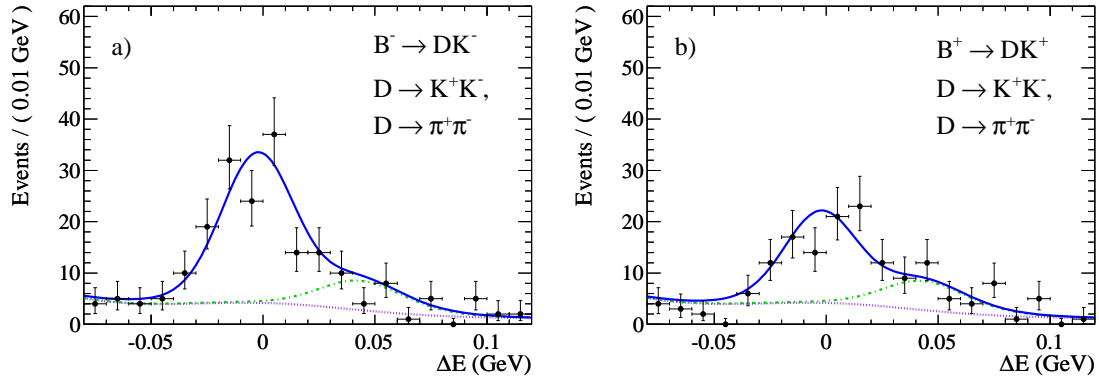


Figure 4:  $\Delta E$  projections of the fits to the data: (a)  $B^- \rightarrow D_{CP+} K^-$ , (b)  $B^+ \rightarrow D_{CP+} K^+$ . The curves are the full PDF (solid, blue), and  $B \rightarrow D\pi$  (dash-dotted, green) stacked on the remaining backgrounds (dotted, purple). We require candidates to lie inside a signal-enriched region:  $0.2 < \mathcal{F} < 1.5$ ,  $5.275 < m_{ES} < 5.285 \text{ GeV}/c^2$ , charged particle from the  $B$  passing kaon identification criteria.

Using a frequentist technique, including statistical and systematic uncertainties, we obtain  $0.24 < r_B < 0.45$  ( $0.06 < r_B < 0.51$ ) and, modulo  $180^\circ$ ,  $11.3^\circ < \gamma < 22.7^\circ$  or  $80.9^\circ < \gamma < 99.1^\circ$  or  $157.3^\circ < \gamma < 168.7^\circ$  ( $7.0^\circ < \gamma < 173.0^\circ$ ) at the 68% (95%) confidence level (Fig. 5). To facilitate the combination of these measurements with the results of the Dalitz-plot analysis, we exclude the  $D \rightarrow K_s^0 \phi$ ,  $\phi \rightarrow K^+ K^-$  channel from this analysis – thus removing events common to the two measurements – and express our results in terms of the variables  $x_\pm$  using  $x_\pm = \frac{1}{4} [R_{CP+}(1 \mp A_{CP+}) - R_{CP-}(1 \mp A_{CP-})]$ . We find:  $x_+ = -0.057 \pm 0.039 \pm 0.015$  and  $x_- = 0.132 \pm 0.042 \pm 0.018$ , in good agreement with the results from the Dalitz-plot analysis.

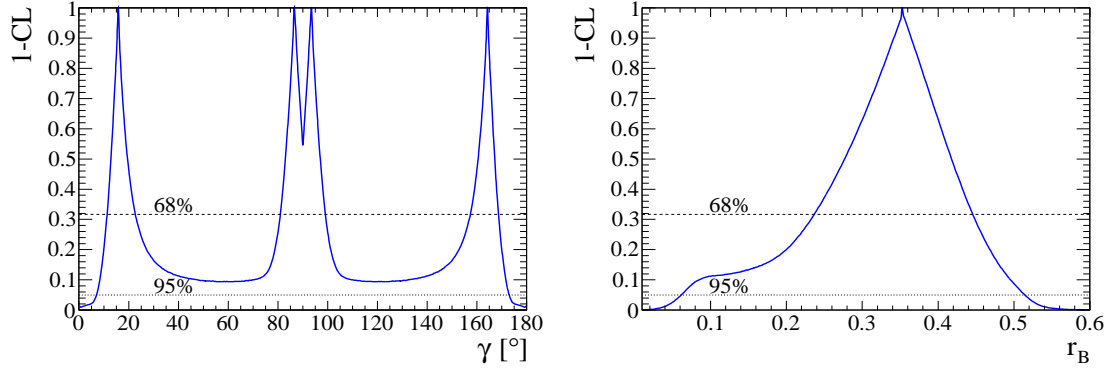


Figure 5: 1-CL as a function of  $\gamma$  mod  $180^\circ$  (left) and  $r_B$  (right) from the  $B \rightarrow DK$  GLW study.

#### 4 ADS method: $B^\pm \rightarrow D^{(*)}K^\pm$ , $D \rightarrow K^\pm\pi^\mp$

We reconstruct  $B^\pm \rightarrow DK^\pm$  and  $D^*K^\pm$  ( $D^* \rightarrow D\gamma$  and  $D\pi^0$ ), followed by  $D$  decays to both the doubly-Cabibbo-suppressed  $D^0$  final state  $K^+\pi^-$  and the Cabibbo-allowed final state  $K^-\pi^+$ , which is used as normalization and control sample [6]. Final states with opposite-sign kaons are produced from the interference of the CKM favored  $B$  decay followed by the doubly Cabibbo-suppressed  $D$  decay and the CKM- and color- suppressed  $B$  decay followed by the Cabibbo-allowed  $D$  decay, and the  $CP$  asymmetries may be potentially very large. On the other hand, their overall branching fractions are very small ( $O(10^{-7})$ ) and background suppression is crucial. The three branching fraction ratios ( $R_{ADS}$ ) between  $B$  decays with opposite-sign and same-sign kaons and the three charge asymmetries ( $A_{ADS}$ ) in  $B$  decays with opposite-sign kaons provide six observables that can be used, together with the measurements by  $c$ - and  $B$ -factories of the amplitude ratio  $r_D$  and the strong phase difference  $\delta_D$  between the two  $D$  decay amplitudes, to determine  $\gamma$  (with a 4-fold discrete ambiguity) and the two sets of  $r_B, \delta_B$  [7].

The yields are determined from fits to  $m_{ES}$  and  $NN$  (Fig. 6). We see indications of signals for the  $B \rightarrow DK$  and  $B \rightarrow D^*_{D\pi^0}K$  opposite-sign modes, with significances of  $2.1\sigma$  and  $2.2\sigma$ , respectively. The measured branching fraction ratios are  $R_{ADS}^{DK} = (1.1 \pm 0.5 \pm 0.2) \times 10^{-2}$  and  $R_{ADS}^{D\pi^0 K} = (1.8 \pm 0.9 \pm 0.4) \times 10^{-2}$ . The  $CP$  asymmetries are large,  $A_{ADS}^{DK} = -0.86 \pm 0.47^{+0.12}_{-0.16}$  and  $A_{ADS}^{D\pi^0 K} = +0.77 \pm 0.35 \pm 0.12$ . We see no evidence of opposite-sign  $B \rightarrow D^*_{D\gamma}K$  decays, and measure  $R_{ADS}^{D\gamma K} = (1.3 \pm 1.4 \pm 0.8) \times 10^{-2}$  and  $A_{ADS}^{D\gamma K} = +0.36 \pm 0.94^{+0.25}_{-0.41}$ . From these results we infer  $r_B^{DK^\pm} = 0.095^{+0.051}_{-0.041}$ ,  $r_B^{D^*K^\pm} = 0.096^{+0.035}_{-0.051}$  and  $54^\circ < \gamma < 83^\circ$  (Fig. 7).

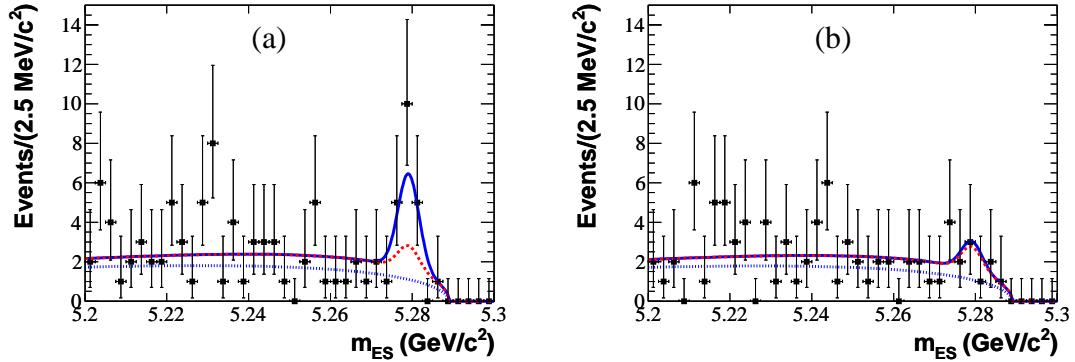


Figure 6:  $m_{ES}$  projection of the fit to the data for the  $B^\pm \rightarrow DK^\pm$ ,  $D \rightarrow K^\mp \pi^\pm$  decays, for samples enriched in signal ( $NN > 0.94$ ), for (a)  $B^+$  and (b)  $B^-$  candidates. The curves represent the fit projections for signal plus background (solid), the sum of all background components (dashed), and the  $q\bar{q}$  background only (dotted).

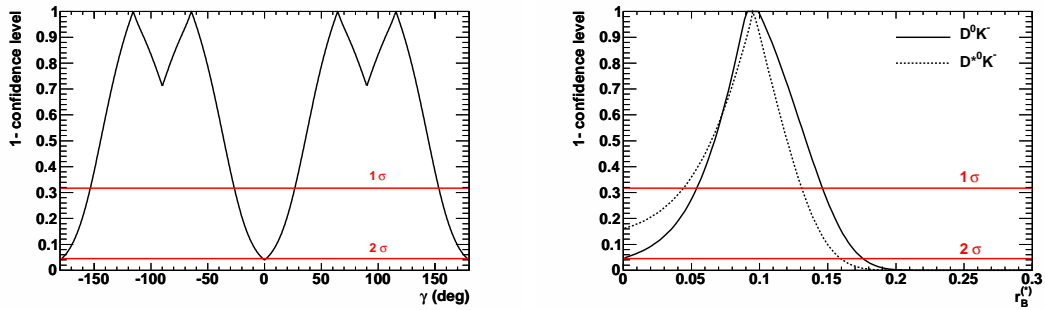


Figure 7: 1-CL as a function of  $\gamma$  (left) and  $r_B$  (right) from the  $B \rightarrow D^{(*)}K$  ADS study.

## 5 Conclusion

The full *BABAR* dataset has been exploited to measure the CKM angle  $\gamma$  in several  $B^\pm \rightarrow D^{(*)}K^{(*)\pm}$  decays using three alternative techniques. A coherent set of results on  $\gamma$  and on the hadronic parameters characterizing the  $B$  decay amplitudes has been obtained. The central value for  $\gamma$ , around  $70^\circ$ , is consistent with indirect determinations from the CKM fits. We attained a precision on  $\gamma$  around  $15^\circ$ , and confirm the theoretical expectations of significant suppression ( $r_B \approx 0.1$ ) of the  $b \rightarrow u$  mediated decay amplitud with respect to the  $b \rightarrow c$  one. Finally, two direct CP violation evidences at the level of  $3.5\sigma$  have been observed.

## References

- [1] P. del Amo Sanchez *et al.* [*BABAR* Collaboration], Phys. Rev. Lett. **105**, 121801 (2010).
- [2] A. Giri, Y. Grossman, A. Soffer and J. Zupan, Phys. Rev. D **68**, 054018 (2003).
- [3] P. del Amo Sanchez *et al.* [*BABAR* Collaboration], Phys. Rev. Lett. **105**, 081803 (2010).
- [4] P. del Amo Sanchez *et al.* [*BABAR* Collaboration], Phys. Rev. D **82**, 072004 (2010).
- [5] M. Gronau and D. Wyler, Phys. Lett. **B265**, 172; M. Gronau and D. London, Phys. Lett. **B253**, 483 (1991).
- [6] P. del Amo Sanchez *et al.* [*BABAR* Collaboration], Phys. Rev. D **82**, 072006 (2010).
- [7] D. Atwood, I. Dunietz and A. Soni, Phys. Rev. Lett. **78**, 3257 (1997).